Gayathri Thangavel, Kavitha Balakrishnan, Nirmala Murugesan*

Department of Physics, Sri GVG Visalakshi College for Women, Udumalpet, India

Scientific paper
ISSN 0351-9465, E-ISSN 2466-2585
https://doi.org/10.62638/ZasMat1120

Zastita Materijala 65 (2)
315 - 330 (2024)

NiO/MnO_2 nanocomposite in addition of layered Reduced Graphene Oxide (RGO) electrode for accountable supercapacitor application

ABSTRACT

(Reduced Graphene oxide/Nickel oxide/Magnesium dioxide) RGO/NiO/MnO_2 nanocomposite electrode was successfully prepared by simple co-precipitation method. The synthesised nanocomposite was characterised by XRD, FESEM, EDAX, FTIR, UV, CV, GCD, EIS. The RGO/NiO/MnO_2 nanocomposite was pretreated by ultrasonication, followed by thermal annealing at 350 ^oC. The crystalline face and size of nanocomposite were analysed by X-Ray Diffraction (XRD). The sandwich-like structure of RGO/NiO/MnO_2 was analysed by Scanning Electron Microscope (SEM). This structure promoted an efficient contact between electrolyte and active materials, and the distinct architecture could offer fast transfer channels of ion and electrons. The nanocomposite exhibited high conductivity owing to the presence of RGO. The electrochemical performance of prepared nanocomposite was done by Cyclic Voltammetry (CV), Galvanostatic charge discharge (GCD), Electrical Impedance Spectroscopy (EIS). The synthesised RGO/NiO/MnO_2 nanocomposite acquired high specific capacitance of 1167F/g at current density of 1 A/g. The low cost, low temperature RGO/NiO/MnO_2 nanocomposite electrode could be the promising electrode for Energy storage devices.

Keywords: *Reduced Graphene Oxide (RGO), NiO/MnO_2 nanocomposite, pseudo- capacitor, cyclic voltammograms, Supercapacitor*

1. INTRODUCTION

Supercapacitors have been in the limelight as a sort of energy storage technology among research groups and business for several decades. However, ongoing advancements in electrode development and manufacture are crucial for producing a low-cost supercapacitor with acceptable electrochemical properties [1] Due to their high-power densities, large specific capacitance, rapid charge-discharge times, long cycle life, and hygienic electrochemical energy storage, supercapacitors (SCs) are the best solution for energy storage technology [2]. Consequently, it is widely stated that improving the electrochemical performance of supercapacitors may be achieved by material synthesis through sustainable synthesis and fabrication methodologies, specifically by changing the structure of the electrode's active components [3]. Electrochemical double-layer capacitors (EDLCs) are made of carbon-based materials (graphene oxide, carbon nanotubes, etc.), but conducting polymers, metal oxides, metal sulphides and conducting polymers are employed in the construction of battery-and/or pseudo capacitive-type cells [4].

Metal oxides like NiO and MnO_2 are among the active materials utilized in pseudo capacitive and/or battery-type applications that are being thoroughly studied and analysed because of their higher chemical stability and eco-friendliness. The composition of these metal oxide-based nanomaterials may offer more active sites and a synergistic effect for improved electrochemical processes [5]. Several attempts have been reported in this context, especially with regard to the synthesis of metal oxide nanostructures. In order to reduce ionic/electronic resistance and shorten ion diffusion paths between the electrode and the electrolyte surface, metal oxides and their nanoscale morphologies are also utilized [6]. When creating pseudo-capacitors, a variety of transition metal oxide nanostructures, including MnO_2, CO_3O_4, V_2O_5, SnO_2, and NiO, are frequently

*Corresponding author: Gayathri Thangavel
E-mail: gayathrithangavel18@gmail.com
Paper received: 03. 12. 2023.
Paper corected: 14.01. 2024,
Paper accepted: 16. 01. 2024.
Paper is available on the website: www.idk.org.rs/journal

utilized as electrode materials. Because of its appealing qualities, including its relative abundance, low cost, strong redox property, large electrochemical surface area, high specific capacitance value, and ease of production, nickel oxide (NiO) can be chosen as an appropriate electrode material among these [7].

NiO's high resistance in electrochemical capacitors is its primary disadvantage. Using highly conductive carbonaceous materials like RGO, graphene, and CNTs can help with this high resistivity issue. Here, by decreasing carbon nanostructure agglomeration and restacking, NiO nanostructures serve as a spacer between various carbon nanostructures and enhance the electrochemical surface area for redox reaction [8]. As a result, the two-dimensional (2D) structure with sp^2 hybridized carbon atoms, such as RGO, is an attractive choice due to its high conductivity, large specific surface area, and robust cycle stability, which can minimize the resistivity of NiO nanoflakes. Many researchers have created RGO-based nanocomposite materials that increase the electrochemical performance of supercapacitors [9]. The development of sophisticated materials with high capacitance and rate capacity is essential to achieve the aforesaid design. Complementary benefits are often produced by a composite that is constructed with the appropriate mix of two components [10]. Everyone knows that because of its high theoretical specific capacitance, huge specific surface area, and extraordinarily high electrical conductivity, reduced graphene oxide (RGO) is one of the most promising electrode materials for EDLCs. When appropriately included into the composite, RGO improves the electrode's structural stability in addition to the composite's electrical conductivity. Consequently, using reduced graphene oxide as a framework is auseful strategy for enhancing the composites' mechanical strengths [11].

Alsaiari et al., reported ZnO/NiO produced specific capacity of 350 F/g was found at 2 A/g current while the lowest specific capacity of 217 F/g was measured at 20 A/g [12]. Mohammad Shariq et al., synthesised nano-composites of (Co_3O_4/NiO), the specific capacitance of which was 2769.2 F/g at 5 mV/s [13]. Geerthana Mummoorthi et al., researched that the ternary composite α-Fe_2O_3/NiO/rGO has shown a specific capacitance of 747 F/g@ a current density of 1 A /g in a 6 M KOH [14]. Qi An et al., prepared NiO-rGO, NiO nanoparticles uniformly distributed in rGO to achieve a high specific capacity at current density of 0.5 A /g[15].O. C. Pore et.al., synthesised NiO/rGO composite achieved the highest specific capacitance of 727.1 F/g at 1 mA cm^{-2} current density and showed good cyclic stability of about 80.4% over 9000 cycles[16]. S.Seenivasan et al., notably, NiO@MnO_2@rGO modified structure exhibited excellent conductivity due to the presence of rGO, demonstrating a high charge storage capacity of 536 F/g at a current density of 1 A/g[17].

RGO (Reduced Graphene Oxide) is effectively integrated in NiO/MnO_2 nanocomposites to make better composites. The co-precipitation approach were used successfully to synthesize the RGO/NiO/MnO_2 composite.

2. EXPERIMENTAL METHOD

2.1. Preparation of RGO/NiO nanocomposite

For preparation of RGO/NiO nanocomposite, 0.01 g of commercially available RGO and 0.1 M of Nickel Nitrate hexahydrate (Ni $(NO_3)_2$.6 H_2O) was taken in 100 ml of deionized water and sonicated for 30 minutes. Then both the solutions were stirred for 2 hours. The pH was then gradually raised to 9 by adding 0.1M of sodium hydroxide (NaOH). After that, the particles were centrifuged with ethanol and deionized water. The particle was first dried for six hours at 150ºC in an oven, and then it was calcined for 2 hours at 350ºC.

Figure 1. Schematic representation of synthesis procedure of RGO/NiO/MnO_2nanocomposite

Slika 1. Šematski prikaz postupka sinteze RGO/NiO/MnO_2 nanokompozita

2.2. Preparation of RGO/NiO/MnO_2 nanocomposite

To prepare the RGO/NiO/MnO_2 Nanocomposite, 0.01 g of RGO, 0.1M Nickel Nitrate hexahydrate Ni $(NO_3)_2.6\ H_2O$ and 0.1M of Manganese acetate tetrahydrate $(CH_3COO)_2Mn\ 4H_2O$ were dissolved in 100 ml of deionised water. Then the solution were sonicated for 30 minutes and stirred for 2 hours. Following that, 0.1 M of Sodium hydroxide (NaOH) was added drop by drop until the pH reached 9. After that, the particle was centrifuged in deionized water and ethanol. The particle was dried in a 150°C oven for 6 hours before being calcinated in muffle furnace at 350°C for 2 hours.

2.3. Characterization

A Shimadzu X-ray diffractometer (D8 ADVANCE) with a vertical goniometer fitted with vanadium filter and copper radiation (CuKα λ=1.54 Å) with a step size of 1.01° was used for the structural analysis of the synthesised nanoparticles. FTIR spectrophotometer, (JASCO) FTIR spectrometer model FT/IR- 4600 series) ranging 500 cm^{-1} to 4000 cm^{-1} was used to determine chemical bonding and functional group present in the synthesised nanoparticles. The Morphological characterization of the synthesized NiO was studied using (Jeol 6390LV) for Scanning Electron Microscopy (SEM) analysis. A JASCO V-770UV double beam spectrophotometer was used for optical studies in the wavelength range 400-2500nm.

2.4. Electrochemical Measurements

The Electrochemical analyses such as cyclic voltammetry, electrochemical impedance, and galvanostatic charge–discharge (GCD) measurements were carried out using an electrochemical workstation (Metrohm AutolabM204) with potential window of -0.1 to +0.5 at room temperature. The electrochemical analysis has been done with three electrode system, specifically, Nickel foam (substrate) was used as a working electrode, Ag/AgCl as reference electrode and Platinum electrode (Pt) electrode as counter electrode.

2.5.. Fabrication of Electrode Material

Preparation of working electrode. RGO, RGO/NiO, RGO/NiO/MnO_2 coated Ni foam, Ag/AgCl, and platinum were used as working, reference, and counter electrode in a three-electrode cell system. All electrochemical studies were carried out in presence of 1 M KOH as electrolyte at room atmosphere. The working electrode was prepared by uniform mixing of NiO nanoparticles (75 wt%), acetylene black (15 wt%), and polyvinylidene difluoride (PVDF) (10 wt%) in 1-methyl-2- pyrrolidinone (solvent) under sonication to obtain slurry. An adequate amount of slurry was used to deposit on Ni foam with coating area of 1× 1 cm^2. Before this process, Ni foam was washed with acid, detergent, ethanol, and deionized water to remove all surface impurities [18]

3. DISCUSSIONS AND FINDINGS

3.1. XRD Analysis

The prepared nanocomposite was investigated by XRD to evaluate the diffraction pattern and crystalline structure of synthesised nanocomposite. The XRD patterns of (a) RGO, (b) RGO/NiO, and (c) RGO/NiO/MnO_2 nanocomposite are shown in Figure 2. From the XRD diffraction pattern (curve a in Figure 2) the identifying peaks for prepared nanocomposites are at 2θ=26.6°and 44.0° corresponding to (002), (100), the pattern of RGO corresponded to carbon peaks [19-22].

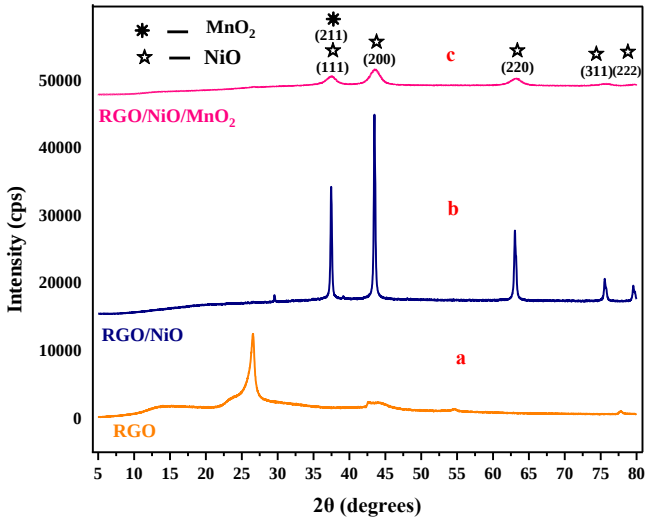

Figure 2. XRD diffractograms of (a) RGO, (b) RGO/NiO, (c) RGO/NiO/MnO_2nanocomposite

Slika 2. XRD difraktogrami (a) RGO, (b) RGO/NiO, (c) RGO/NiO/MnO_2 nanokompozita

Observed peak position for the RGO/NiO nanocomposite (curve b in Figure 2) with 2θ values of 37.45°, 43.437°, 63.05°, 75.56° and 79.52° were indexed on the (111), (200), (220), (311) and (222) NiO crystal planes, respectively (JCPDS Sheet No. 78- 0429) [23]. The absence of additional peaks in the XRD spectrum indicates the purityof the synthesized nanocomposite. No peaks were found at about 26°, indicating thatall graphite powder was oxidized and that the RGO was free of impurities or unreacted graphite [24]. All diffraction peaks were assigned to the centered cubic phase of NiO (FCC), with the lattice constant "a" calculated to be average 4.1634 Å [25].

From (curve c in Figure 2 RGO/NiO/MnO_2 nanocomposite's XRD peaks with 2θ values of 37.45º, 43.54º, 63.15º, 75.64º and 79.58º were indexed to (111) and (211), (200), (220), (311) and (222) respectively [26-28]. When compared to(curve b in Figure 2) the peak's intensity (reduction in height down the y axis) and width both decreased in (curvee c in Figure 2.) [29-33]. This confirmed the development of the NiO, MnO_2, and RGO nanocomposite successfully. And as strain and dislocation density increase, crystalline size decreases [34, 35]. Structural parameters of synthesised RGO, RGO/NiO, RGO/NiO/MnO_2 nanocomposites are calculated using below formulas (1-4) [36] and its structural parameters listed in table 1.

From the observed 'd' spacing and (hkl) planes the lattice constant is evaluated using the relation

$$d = \frac{a}{\sqrt{h^2 + k^2 + l^2}} \quad (1)$$

Where

d — interplanar spacing, and *a* — lattice constant, (hkl planes). From the observed 'd' spacing various structural parameters such as lattice constant, crystalline size, dislocation density and strain have been estimated using the expressions,

The crystalline size of nanoparticles is determined using Debye Scherrer' relation.

$$D = \frac{K\lambda}{\beta \cos\theta} \quad (2)$$

Where

β is the full width half- maximum value of the high intensity peak, θ is Bragg's angle, *K* is the shape factor (K= 0.94) and λ is the wavelength (1.54 A°) of the X-ray source used in the XRD. The crystal structure of the samples is FCC.

The dislocation density (δ) can be calculated using the equation

$$\delta = \frac{1}{D^2} \quad (3)$$

The micro strain (ε) can be calculated using the equation

$$\varepsilon = \frac{\beta \cos\theta}{4} \quad (4)$$

Table.1. Structural parameters of synthesised RGO, RGO/NiO, RGO/NiO/MnO_2 nanocomposites

Tabela 1. Strukturni parametri sintetizovanih RGO, RGO/NiO, RGO/NiO/MnO_2nanokompozita

Composite	2θ values (deg)	hkl	Crystallinesize D (nm)	d value	Lattice constant a (Å)	Micro-strain (ε) 10^3	Dislocation density (δ) 10^{15}L/m^2
RGO	26.32	(002)	3.90	3.0775	-	-	-
RGO/NiO	37.46 43.49 62.05 75.62 79.61	(111) (200) (220) (311) (222)	27.4261 25.7554 17.1699 12.7043 12.1251 Average=19.0362	2.3991 2.0794 1.4733 1.2565 1.2033	4.155 4.158 4.171 4.165 4.168 Average=4.1634	2.4845 2.8801 5.4945 11.6322 14.8890	0.0364 0.0388 0.0582 0.0787 0.0824
RGO/NiO/MnO_2	37.45 43.54 63.15 75.64 79.58	(111)and (211) (200) (220) (311) (222)	4.1450 4.1806 3.9405 3.8884 11.100 Average=5.4509	2.3997 2.0768 1.4710 1.2561 1.2036	4.156 4.154 4.160 4.166 4.173 Average=4.1618	17.0634 19.2870 27.2288 30.6474 10.9880	0.2412 0.2425 0.2537 0.2571 0.0901

3.2. FT-IR spectroscopy

Figure 3. displays FT-IR spectra of the RGO, RGO/NiO, and RGO/NiO/MnO_2 nanocomposite materials. The transmission maxima found in the electromagnetic spectrum between 400 and 4000 cm^{-1} wave numbers. From (curve a in Fig.3) for RGO the C=O stretching vibrations are a result of the 1741.41 cm^{-1} peak. Stretching of the C-O and O-H bonds is shown by the peak at 1369.21 cm^{-1} in the carboxylic group, whereas stretching of the C-O-C bonds is indicated by the peakat 1221.68 cm^{-1} in the epoxy group [37]. In RGO/NiO nanocomposite (curve b in Figure 3), the peaks at 444 cm^{-1} and 673.99 cm^{-1} are associated with Ni-O stretching vibrations, confirmed that NiO nanoparticles were present in RGO [38]. In(curve c in Figure 3) RGO/NiO/MnO_2 two distinct bands at 433 cm^{-1} and 532 cm^{-1} confirm the creation and formation of the MnO_2/NiO nanocomposite. It is also observed that the peak intensity is significantly lower in (curve c in Fig .3) than in (curve b in Figure 3) [39].

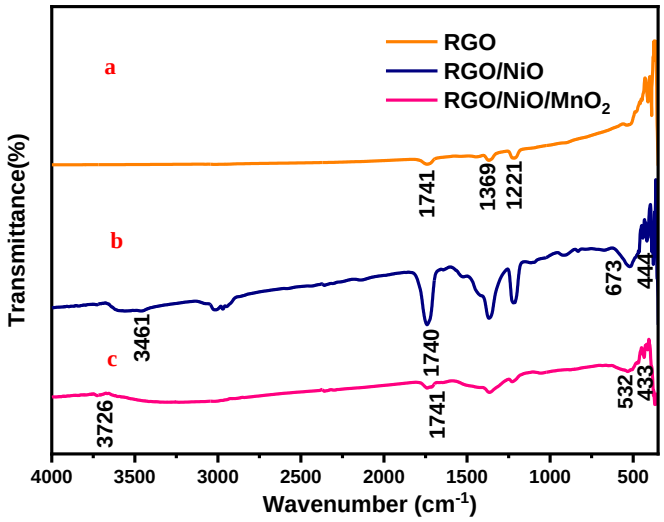

Figure 3. FT-IR spectra of (a) RGO, (b) RGO/NiO, (c) RGO/NiO/MnO_2 nanocomposite

Slika 3. FT-IR spektri (a) RGO, (b) RGO/NiO, (c) RGO/NiO/MnO_2 nanokompozita

3.3. UV-Vis spectroscopy

The optical bandgap energy was estimated from the UV–Vis spectrum using thefollowing (5)

$$\alpha = A(E_g - h\ )^n/hv \qquad (5)$$

For a straight transition, n equals 2, A is a constant, Eg is the bandgap, and α is the absorption coefficient. The bandgap was determined using a plot of $(\alpha hv)^2$ vs photon energy (αhv). The UV-visible absorption spectra of RGO, RGO/NiO, and RGO/NiO/MnO2 are shown in Fig. 4. The intercept of the tangent (tauc plot) to the figure best approximates the bandgap energy for this direct bandgap in Fig. 5. From (curve a in fig .4) displays the RGO absorbance spectrum, which has only one peak at a wavelength of 268 nm and peak has a π-π* transitional orbital correlation [40]. When the wavelength is longer, the absorbance is constant and resembles pure monolayer graphene. Around (curve a in Fig.5) depicts the tauc plot of the RGO and reveals that the bandgap is 3.25 eV.

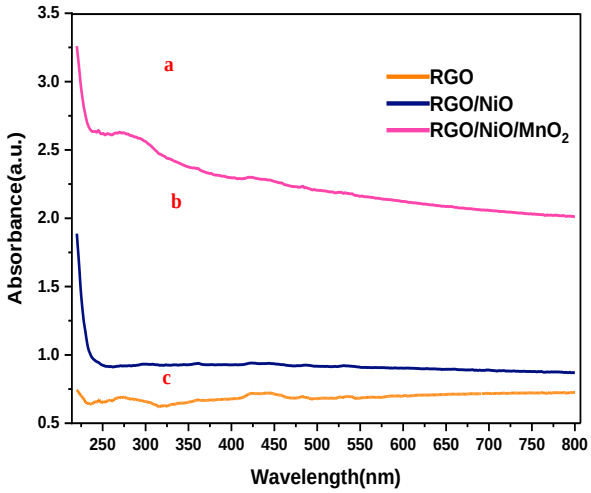

Figure 4. UV-vis absorption spectra of (a) RGO, (b) RGO/NiO, (c) RGO/NiO/MnO_2nanocomposite

Slika 4. UV-vis apsorpcioni spektri (a) RGO, (b) RGO/NiO, (c) RGO/NiO/MnO_2nanokompozita

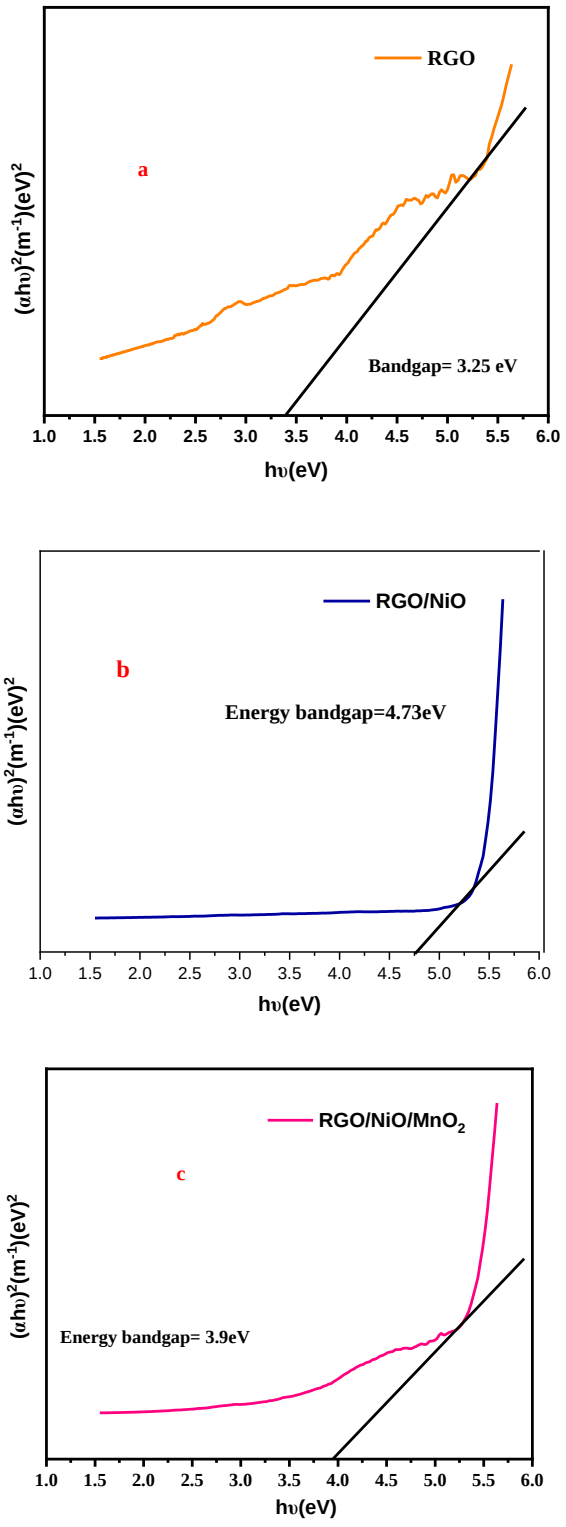

Figure 5. Method for calculating band gap energy (Eg) from the Tauc plot. (a) RGO, (b)RGO/NiO, (c) RGO/NiO/MnO_2 nanocomposite

Slika 5. Metoda za izračunavanje energije širine pojasa (Eg) iz Tauc grafikona. (a)RGO, (b) RGO/NiO, (c) RGO/NiO/MnO_2 nanokompozit

The (curve b in Figure 4) shows the absorbance spectra of RGO/NiO. There was an absorption peak at around 200 nm as a result of direct stimulation of the NiO. The enhanced absorption is due to the chemically decreased material. Based on tauc plot (curve b in Figure 5) the estimated bandgap of RGO/NiO was determined to be 4.73 eV [41]. The largest absorption peak is seen in (curve c in Figure 4), a blueshift (below 300 nm) with the near-visible region's (300–400 nm) peak of RGO/NiO/MnO_2 composite [42]. From (curve c in Figure 5) the bandgap of RGO/NiO/MnO_2 was determined to be 3.9 eV.

3.4. Scanning electron microscopy

The morphological investigation of the synthesized nanocomposite were studied using SEM analysis. The SEM micrographs of the RGO(a–b), RGO/NiO(c– d), and RGO/NiO/MnO_2 nanocomposites (e–f) are shown in Fig. 6. The RGO's morphology shows a collection of thin, transparent sheets separated with a layer in between each sheet. The (image a,b in Fig. 6) shows the randomly distributed waves of silk-like RGO are seen. The RGO sheets' contact resulted in a sequence of minuscule waves. RGO takes on a structure akin to a membrane fold when Van der Wall contact is present, and RGO also seems to be more transparent and squashier. [43].

In the (image c,d in Figure 6) the NiO is a non-uniform, spherical ball-like substance, and its whole structure is composed of a smooth surface measuring around 40nm. It is evident that RGO is essentially transparent and that layers of RGO work together to form a 3D network with plenty of holes in it. SEM images of the two materials compared to one another show that the surface of the RGO/NiO nanocomposite is significantly rougher than that of RGO, which can be attributable to the homogeneous distribution of NiO nanoparticles on RGO [44]. In (image e,f in Figure 6) The cross-section SEM pictures of the manufactured RGO/NiO/MnO_2, show the sandwich-like structure. NiO and RGO are incorporated in the RGO/NiO/MnO2 nanocomposite, and the particle size is determined to be around 17 nm [45].

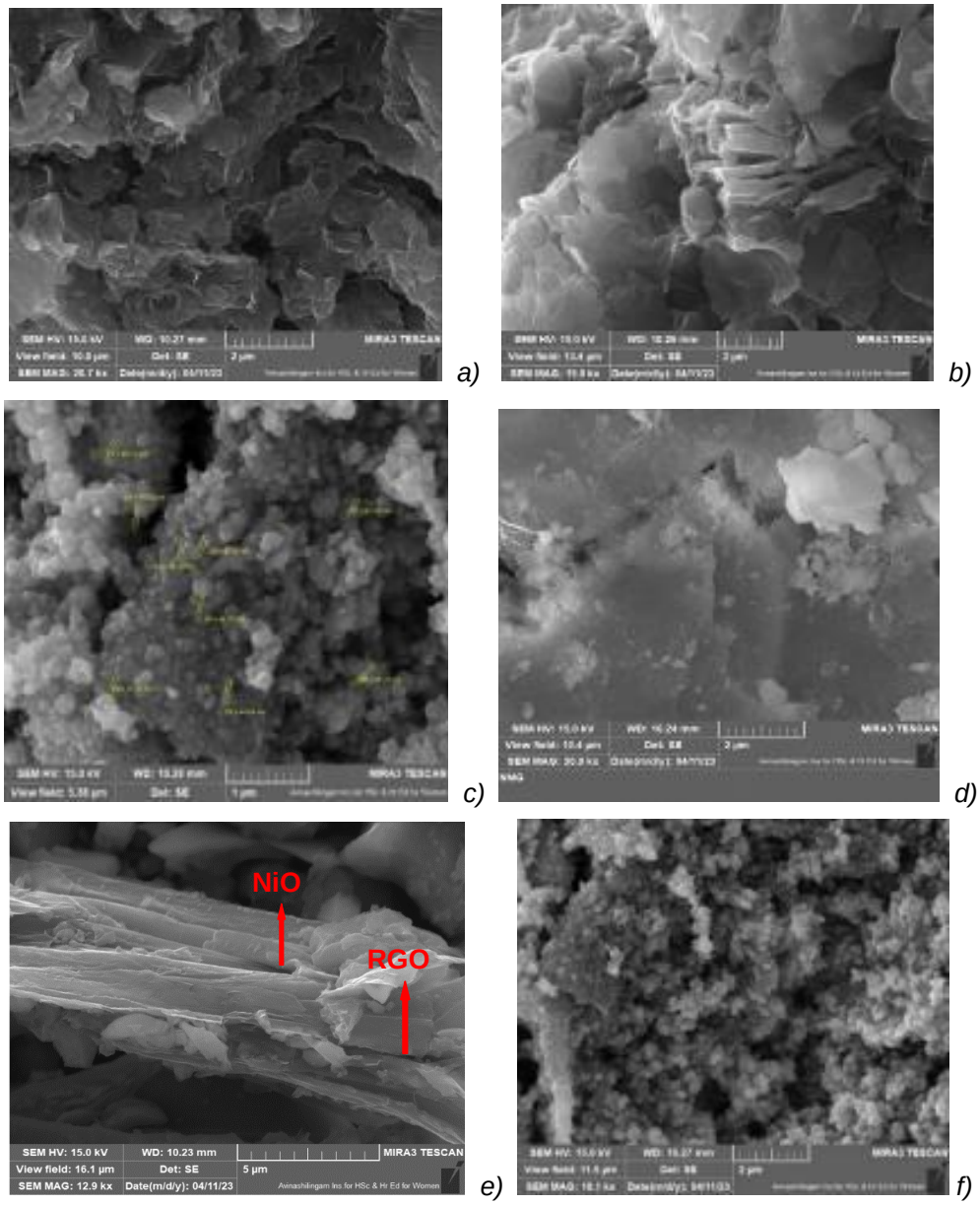

Figure 6. SEM micrographs of (a-b) RGO, (c-d) RGO/NiO, (e-f)RGO/NiO/MnO_2 nanocomposites

Slika 6. SEM mikrofotografije (a-b) RGO, (c-d) RGO/NiO, (e-f)RGO/NiO/MnO_2 nanokompozita

3.5. Energy-dispersive X-ray spectroscopy

Figure 7.represents the elemental distribution (EDAX) and mapping plots for (a)RGO, (b) RGO/NiO, and (c) RGO/NiO/MnO_2electrodes. The Graph a in Figure 7 shows the elemental mapping and EDS spectra of RGO and reveals the presence of the elements O and C, confirming the phase purity of the material. Research on the constituent constituents of RGO confirms their existence and excludes the possibility of any impurities [46, 47].

Graph b in Figure 7 shows the EDAX and Elemental mapping of a RGO/NiO sample, which revealed the presence of C (from the RGO), O (from the NiO), and Ni (from the NiO and RGO). The sample's elemental mappings show that C, O, and Ni are all scattered in the same location, confirming the presence of the NiO/RGO nanocomposite [48]. The graph c in Figure 7 displays the EDAX and Elemental mapping of a RGO/NiO/MnO2 sample, demonstrating the presence of Mn-7.94%, Ni- 49%, C-20.81%, O-19.63%, and other elements due to environmental variablesduring the synthesis process [49].

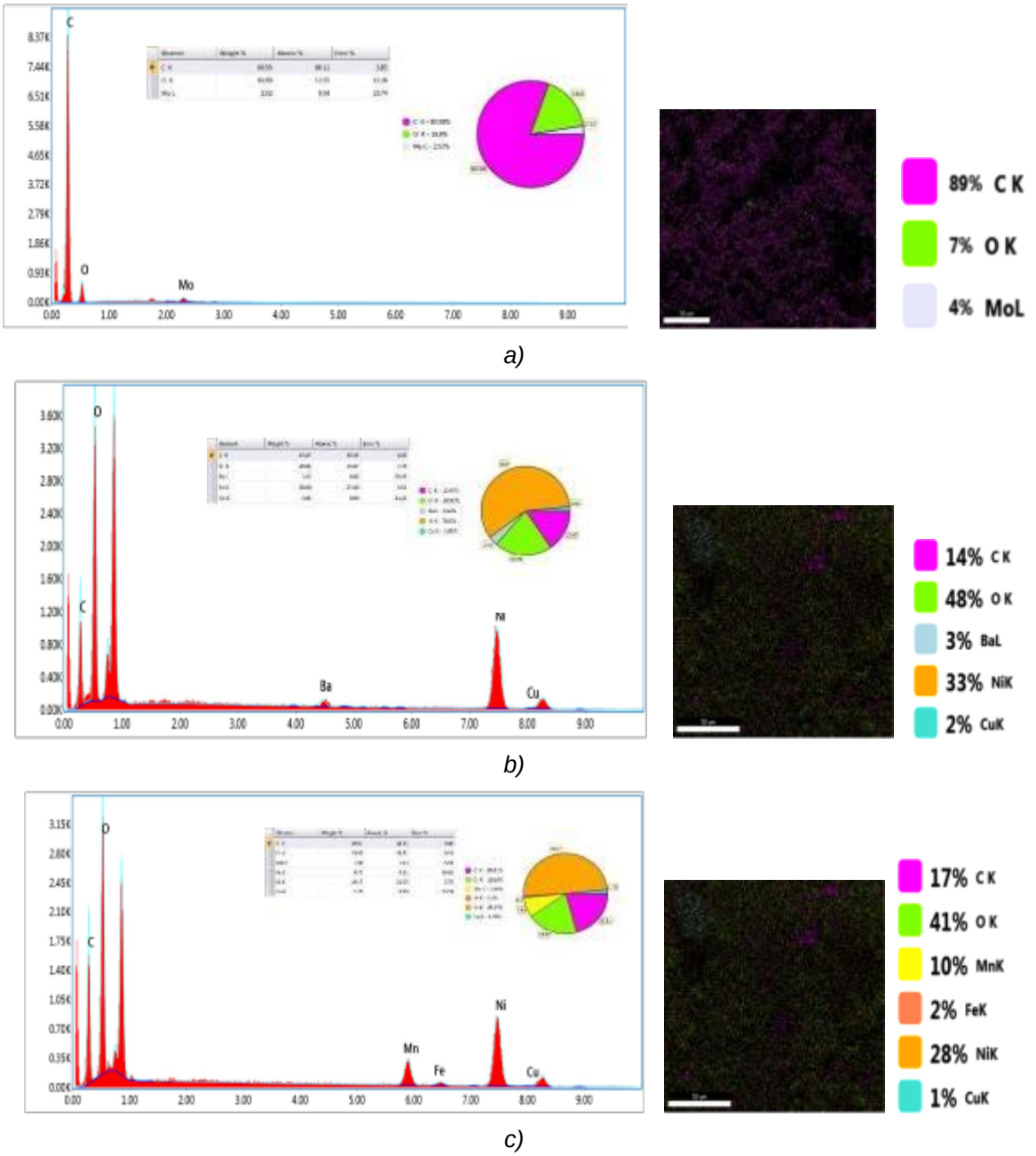

Figure 7. EDS and Elemental mapping of (a)RGO, (b)RGO/NiO, (c) RGO/NiO/MnO_2

Slika 7. EDS i elementarno mapiranje (a)RGO, (b)RGO/NiO, (c) RGO/NiO/MnO_2

4. ELECTROCHEMICAL ANALYSIS

4.1.bCyclic Voltammetry (CV)

Figure 8 depicts cyclic Voltammograms of (a) RGO, (b) RGO/NiO, and (c) RGO/NiO/MnO_2 nanoparticles. In (curve a in Figure .8) Electrochemical experiments were performed on the RGO.RGO electrode CV curves acquired at various scan rates (5, 10, 20, 30, 40, 50, 70, 80, 100, 120, 160, and 320 mV/s) in 1 M KOH electrolyte. The electrode displayed two significant peaks on the anodic and cathodic sides, indicating typical pseudo capacitive behaviour in relation to RGO's faradaic redox reaction.

As a result of electron transport restriction, RGO on the electrode surface generated semi-irreversible behaviour. Surprisingly, the redox peaks of the RGO sample are enhanced due to lattice structures, as shown by the creation of easily reducible oxygen species, resulting in better electrocatalytic performance. Both the cathodic and anodic peak currents increased considerably [50].

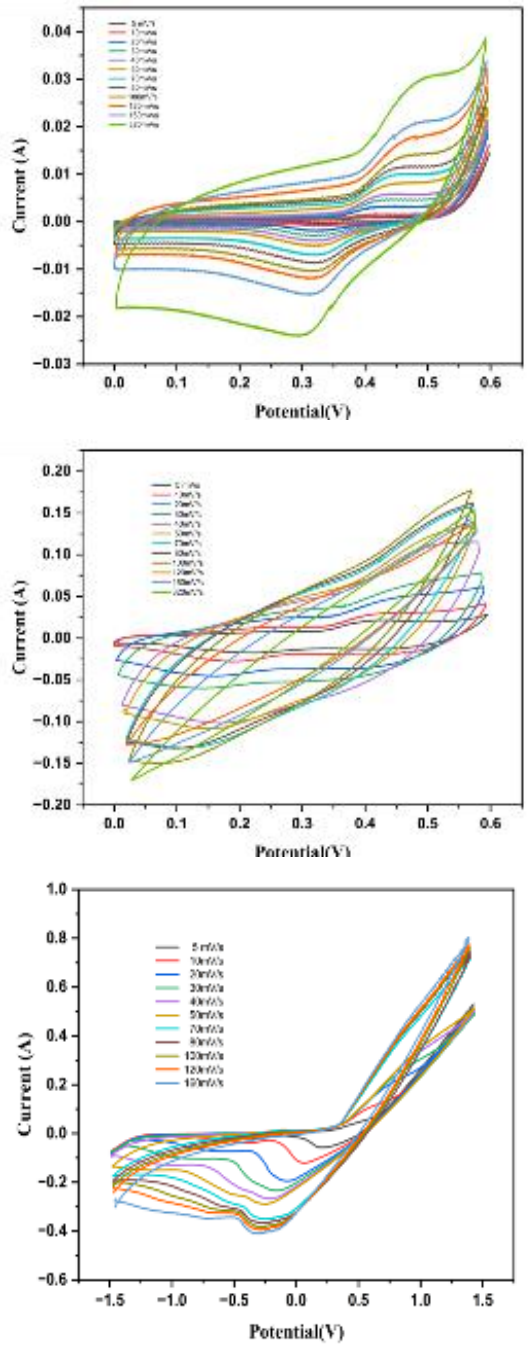

Figure 8. Cyclic Voltammograms of (a) RGO, (b) RGO/NiO, (c) RGO/NiO/MnO_2nanoparticles.

Slika 8. Ciklični voltamogrami (a) RGO, (b) RGO/NiO, (c) RGO/NiO/MnO_2 nanočestica

In (curve b in Figure 8) two reduction peaks and one oxidation peak appear at low scan rates of (5-40mV/s), while at high scan rates of (50-320)mV/s), all curves are inclined, indicating a tremendous potential shift due to one or more types of polarizations that makes the equilibrium potential difficult to distinguish [51].

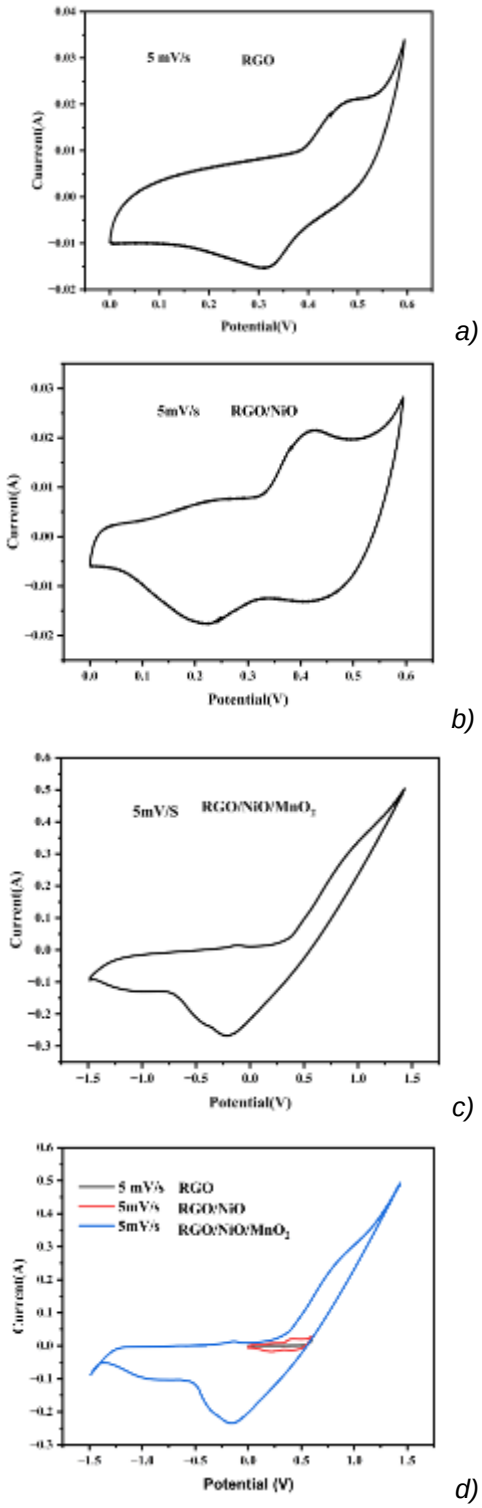

Figure 9. Shows the cyclic voltammograms at 5mV/s scan rate (a) RGO, (b) RGO/NiO, (c) RGO/NiO/MnO_2, (d) combination of RGO, RGO/NiO, RGO/NiO/MnO_2 at 5mV/s scan rate

Slika 9. Prikaz ciklične voltamograme pri brzini skeniranja od 5mV/s (a) RGO, (b) RGO/NiO, (c) RGO/NiO/MnO_2, (d) kombinacija RGO, RGO/NiO, RGO/NiO/MnO_2 pri 5mV/s brzina skeniranja

The RGO/NiO/MnO_2 electrode's CV curve (curve c in Figure 8) clearly displays redox peaks, proving that it is a battery electrode. The peaks showed the Ni and Mn ion redox transition brought on by non-capacitive faradaic behavior. The electrolyte diffusion in the material is responsible for the redox peaks, suggesting that the RGO/NiO/MnO_2 electrode was operating like a battery. The electrode redox behavior, which was based on the Nernstian process, is described by the peak-shaped CV curves. Distinct redox peaks were seen at high scan speeds, suggesting that the working electrode had strong reversibility and a high rate of capability.

Figure 9 displays the cyclic voltammograms at 5mV/s scan rate (a) RGO, (b) RGO/NiO, (c) RGO/NiO/MnO_2, and the (curve d in Fig.9) shows the combination of RGO, RGO/NiO, and RGO/NiO/MnO_2 RGO, RGO/NiO electrodes in the 0 to 0.6 V range and RGO/NiO/MnO_2 electrodes in the -1.5to +1.5V range at a scan rate of 5 mV/s, respectively. Each curve had redox peaks. These findings showed that the capacitive process was regulated by faradaic reactions. Furthermore, the integral areas of the materials were in the order RGO< RGO/NiO< RGO/NiO/MnO_2, suggesting that the composite electrode outperformed the other electrodes in terms of capacitance performance.

4.2. Galvanostatic Charge/Discharge (GCD)

Figure 10 depicts the galvanostatic charge-discharge curves of (a) RGO, (b) RGO/NiO,and (c) RGO/NiO/MnO_2. For different current densities (1, 1.5, 2, 2.5, 3, and 3.5) at potentials ranging from -0.1 to 0.5 V in 1 M KOH electrolyte [53]. In Figure 10, the discharge time decreased as the current density increased. These semi symmetric discharge curves corroborate the pseudo capacitive nature of the a) RGO, b) RGO/NiO, and c) RGO/NiO/MnO_2 electrodes [54].

It is hypothesized that there is a redox reaction at the electrode-electrolyte interface. The specific capacitance of the a) RGO, b) RGO/NiO, and c) RGO/NiO/MnO_2 electrodes was calculated using equation (6) [55,56]. In table .2 calculated specific capacitance corresponding current densities of RGO, RGO/NiO, and RGO/NiO/MnO_2 are shown.RGO/NiO/MnO_2 show high Specific capacitance of 1167 F/g at current density 1A/g. Calculated using below Eq .6 were C_s = specific capacitance (F /g), I= (A /g) is the applied current density, Δt (s) is the discharging time, ΔV (V) is the maximum potential window to discharge the cell.

$$C_s = \frac{(1+\Delta t)}{(\Delta V x m)} \qquad (6)$$

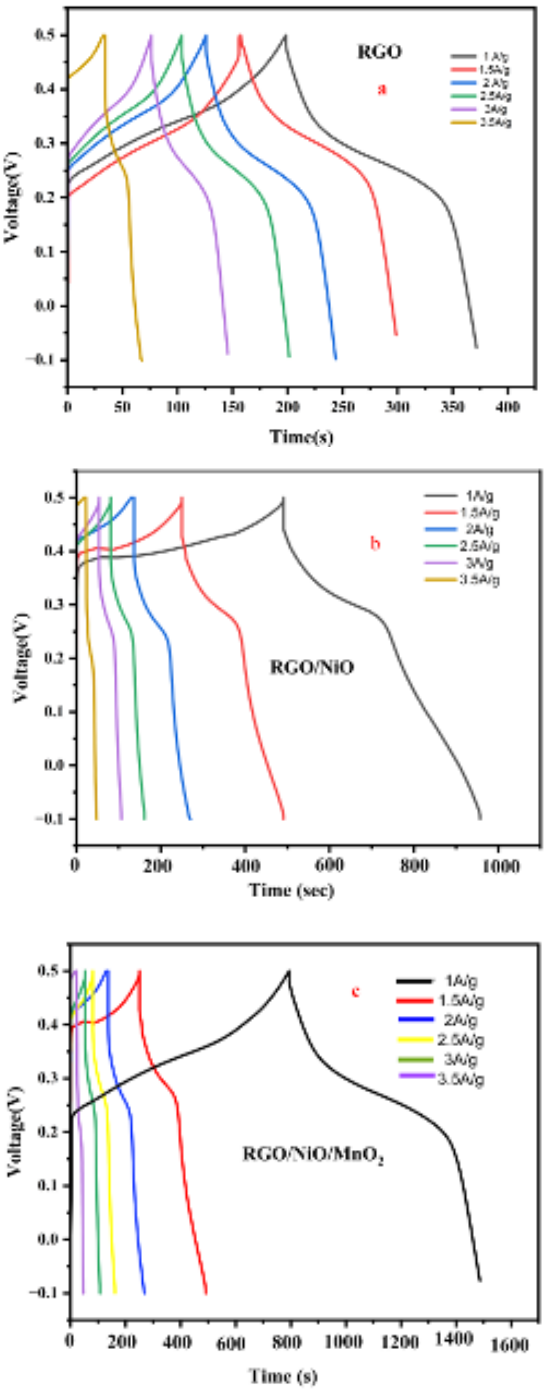

Figure 10. Galvanostatic charge/discharge of (a) RGO, (b) RGO/NiO, (c) RGO/NiO/MnO_2

Slika 10. Galvanostatsko punjenje/pražnjenje (a) RGO, (b) RGO/NiO, (c) RGO/NiO/MnO_2

Figure 11 depicts the curve of specific capacitance versus discharge current densities for all electrodes. At low current density, the specific capacitance value is maximum, and it decreases at high current density. The electrode discharges faster at high current densities, resulting in a low specific capacitance value, whereas the electrode

discharges slowly at low current densities, resulting in a high Cs. Cs decreases at high current density and scan rate due to poor electrolyte ion transport. Because only the outer active surface is employed for charge storage, and because time is limited during the high-rate charge-discharge process and ionic mobility in the electrolyte is always regulated by diffusion.

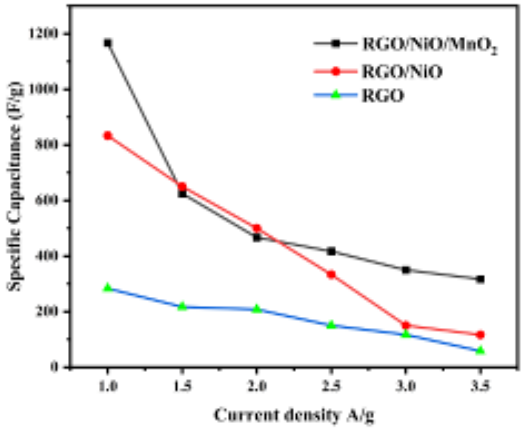

Figure 11. Comparison specific capacitance versus discharge current for Galvanostatic charge/discharge of RGO, RGO/NiO, RGO/NiO/MnO_2

Slika 11. Poređenje specifične kapacitivnosti u odnosu na struju pražnjenja zagalvanostatičko punjenje/pražnjenje RGO, RGO/NiO, RGO/NiO/MnO_2

Table 2. Calculation of specific capacitance at different current densities

Tabela 2. Proračun specifične kapacitivnosti pri različitim gustinama struje

Current density (A/g)	Specific capacitance (F/g)		
	RGO	RGO/NiO	RGO/NiO/MnO_2
1	283	833	1167
1.5	217	625	625
2	208	500	467
2.5	150	333	417
3	117	150	350
3.5	58	117	317

4.3 .Electrochemical Impedance Spectroscopy (EIS)

EIS measurements were used to understand the interfacial chargetransfer process. Furthermore, electrochemical impedance spectroscopy measurements in the frequency range of 0.01 Hz to 100kHz were acquired from the EIS plots and the related equivalent electrical circuit of Nyquist plot of EIS of RGO, RGO/NiO, RGO/NiO/MnO_2 nanocomposite are shown in (curve a,b,c in Figure 12). In (curve a in Figure .12) There is no semi-circular area in the Nyquist plot and Electron transfer between electrodes is boosted by RGO therefore RGO's conductivity is clearly high [57]. This is due to the restoration of RGO's graphitic nature (i.e., sp_2 bonds). It is noted that the diameter grew in (curve c in Figure 12) compared to (curve b in Figure 12) [58]. The (curve b,c in Figure 12) depicts the EIS curves in the high frequency zone, demonstrating that both semicircles are almost coincident, indicating that the electrolyte resistance and charge transfer resistance of the RGO/NiO/MnO_2 nanocomposite are similar [59].

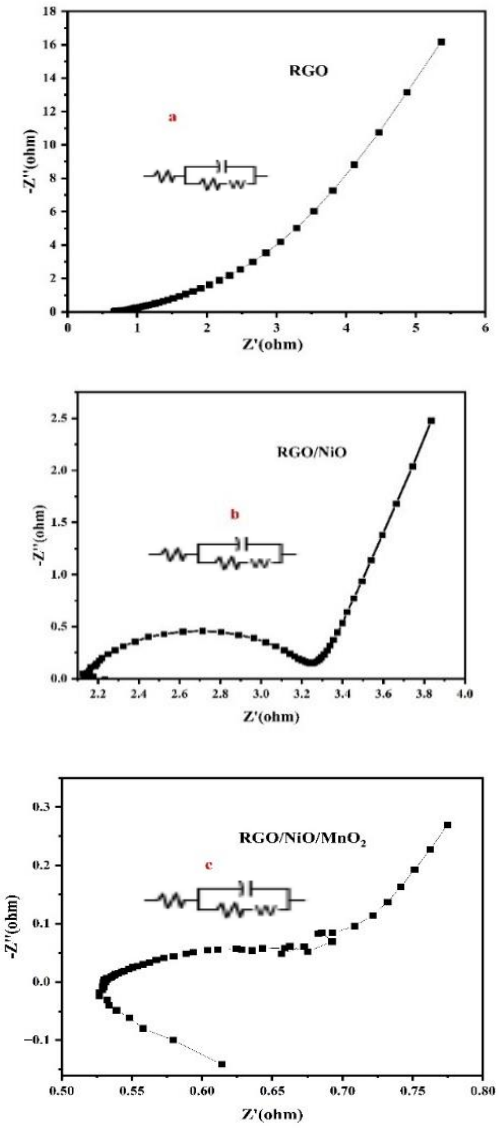

Figure 12. EIS Nyquist plot of (a) RGO, (b) RGO/NiO, (c) RGO/NiO/MnO_2

Slika 12. EIS Najkvist dijagram (a) RGO, (b) RGO/NiO, (c) RGO/NiO/MnO_2

Table 3. Comparison of the maximum capacitance values of the reported electrodes and the present electrode (RGO/NiO/MnO_2 nanocomposite)

Tabela.3. Poređenje maksimalnih vrednosti kapacitivnosti prijavljenih elektroda i sadašnje elektrode (RGO/NiO/MnO_2 nanokompozit)

Electrode material	Capacitance (F /g)	Ref.
1. Binary MnO2–NiO oxides	160 (50 mV /s)	60
2. Porous nickel manganite composites	180 (0.25 A /g)	61
3. Nanosized Ni–Mn oxides	195 (10 mV /s)	62
4. Mn/Ni mied oxidexs	210 (0.12 A /g)	63
5. Nickel-manganese oxide	284 (5 mV /s)	64
6. Ni(OH)2–MnO2 core–shell nanostructures	355 (0.5 A /g)	65
7. Mesoporous Mn–Ni oxides	411 (2 mV /s)	66
8. Nanostructured NiO–MnO2 composite	453 (10 mV /s)	67
9. Graphene–MnO2 nano wall hybrids	122 (10 mV /s)	68
10. Graphene–MnO2–carbon nanotubes	193 (0.2 A /g)	69
11. Graphene-honeycomb-like MnO2	210 (0.5 A /g)	70
12. Hydrothermally reduced graphene–MnO2	212 (2 mV /s)	71
13. Graphene porous NiO nanocomposite	430 (0.2 A /g)	72
14. RGO/NiO/MnO2 nanocomposite	1167 (1 A/g)	Present work

5. CONCLUSION

A RGO/NiO/MnO_2 nanocomposite was successfully synthesized by co- precipitation technique. The crystallographic, surface morphology, optical studies and capacitive behaviour of the nanocomposite were studied. Incorporation of RGO shows nanosheet like structure which is used not only to enhance the stability of NiO and MnO_2 but also to improve the electrochemical reactions of the nanocomposite electrode material. This behaviour resulted from the uniform distribution of NiO/MnO_2 on RGO nanosheets. This uniform morphology and the higher conductivity of the composite facilitate electrolyte diffusion and electron transfer in the nano-composite materials. The RGO/NiO/MnO_2 nanocomposite showed a highest specific capacitance of 1167 F/g at a current density of 1 A/g representing excellent electrochemical performance. Therefore, the results proved that the composite electrode material can be used as an active electrode material for supercapacitor application.

Acknowledgement

The authors are grateful to the Secretary, Director, Principal and Head of the Department of Physics, Sri G.V.G Visalakshi College for Women, Udumalpet for their excellent encouragement and support and Prof.C.N.R Rao Research Centre, Avinashilingam university, Coimbatore, Tamil Nadu, India. This research did not receive any specific grant from funding agencies in the public, commercial, or not- for-profit sectors.

Compliance with ethical standards

Conflict of interest *the authors declare that they have no conflict of interest.*

6. REFERENCE

[1] N.A.Salleh, S.Kheawhom, N.A.A.Hamid (2023) Electrode polymer binders for supercapacitor applications: A review, J. of materials research and technology.,23, 3470-3491. https://doi.org/10.1016/ j.jmrt.2023.02.013

[2] S.Kalaiarasi, S.Shyamala, M.Kavitha (2022) Electrochemical performance of r- graphene oxide based MnO_2 nanocomposite for supercapacitor, nanosystems: Phys. Chem. Math., 13 (3), 320–330. DOI http://dx.doi.org/10.17586/2220-8054-2022-13-3-320-330

[3] S.J.Park, Y.R.Son, Y.J.Heo (2018) Prospective Synthesis Approaches to Emerging Materials for Supercapacitor, Emerging Materials for Energy Conversionand Storage.,6,185-208. https://doi.org/ 10. 1016/B978-0-12- 813794-9.00006

[4] C.An, Y.Zhang, H.Guo, Y.Wang (2019) Metal oxide-based supercapacitors: progress and prospectives, Nanoscale Advances., 12, 4644-4659. https://doi.org/10.1039/C9NA00543A

[5] R.Kumar, R.Thangappan (2022) Electrode material based on reduced graphene oxide (rGO)/transition metal oxide composites for supercapacitor applications: a review, Emergent Materials .,5, 1881–1897. https://doi.org/10. 1007/s42247-021-00339-7

[6] S.Tamang, S.Rai, R.Bhujel (2023) A concise review on GO, rGO and metal oxide/rGO composites: Fabrication and their supercapacitor and catalytic applications, Journal of Alloys and Compounds., 947, 169588. https://doi.org/10. 1016/ j.jallcom.2023.169588.

[7] S.Rusi , R.Majid (2015) Green synthesis of in situ electrodeposited rGO/MnO2 nanocomposite for high energy density supercapacitors, *Sci Rep* **5.**, 16195. https://doi.org/10.1038/srep16195

[8] R.Rajeswari, A.Kavitha, B.Ananda, P.H. Gurumallesh (2021) A Review on Graphene Based Metal/Metal Oxide Composites and Enhanced Properties along with Biomedical Applications, Nano Res Appl .,7,3-6. doi: 10.1007/s40820-018-0206-4

[9] S.M.Majhi, A.Mirzaei, H.W.Kim, S.S.Kim (2021) Reduced Graphene Oxide (rGO)-Loaded Metal-Oxide Nanofiber Gas Sensors: An Overview, Sensors (Basel)., 21(4), 1352. https://doi.org/ 10.3390%2Fs21041352

[10] S.Yadav, N.Rani, K.Saini (2022) A review on transition metal oxides based nanocomposites, their synthesis techniques, different morphologies and potential applications, IOP Conf. Ser.: Mater. Sci. Eng., 1225 012004.doi:10.1088/1757- 899X/1225/ 1/012004

[11] D.Selvakumar, P.Nagaraju, R.Jayavel (2018) Graphene-Metal Oxide based Nanocomposites for Supercapacitor Applications. Advanced Materials: TechConnect Briefs., p.70—73.Graphene-Metal Oxide Based Nanocomposites for Supercapacitor Applications

[12] N. S.Alsaiari, M.Ahmad, I.Shaheen, I. Ali , U.Amara (2023) Three-dimensional flower-like nanocomposites based on ZnO/NiO as effective electrode materials for supercapacitors, Journal of Electroanalytical Chemistry., 930, 11715. https://doi.org/10.1016/j.jelechem.2023.117158

[13] M.Shariq, A. BaQais, T.M.Althagafi, O.Madkhali, A. A.Alholaisi, S.Hussain , Y.Javed (2023) Synthesis of Co_3O_4/NiO nanospherical composites as electrode material for high-performance supercapacitors, Eur. Phys. J. Plus., **138**, 389 . https://doi.org/10.1140/epjp/s13360-023-04001-5

[14] G.Mummoorthi, S.Shajahan, M.A.Haija, U. Mahalingam, R.Rajendran (2022) Synthesis and Characterization of Ternary α-Fe_2O_3/NiO/rGO Composite for High- Performance Supercapacitors, ACS Omega., 7, 31, 27390–27399. https://doi.org/10.1021/acsomega.2c02418

[15] Q.An, X.Zhao, S.Bai (2021) Novel Lithium-Ion Capacitor Based on a NiO-rGO Composite, Materials ., 14(13),3586. https://doi.org/10.3390/ ma14133586

[16] O.C.Pore, A.V.Fulari, V.G.Parale, H.H.Park, R. V. Shejwal, V.J.Fulari, G.M.Lohar (2022) Facile hydrothermal synthesis of NiO/rGO nanocomposite electrodes for supercapacitor and nonenzymatic glucose biosensing application. **J**.of Porous Materials., 29(6), 1991-2001. https://doi.org/ 10.1007/s10934-022-01313-2

[17] S.Seenivasan, S.Dhinesh, F.Maiz, M.Shkir (2023) Electrochemical investigation of NiO@MnO_2@rGO ternary nanocomposite-based electrode material for high-performance supercapacitor applications, Ionics., **29**, 3641–3652. https://doi.org/10.1007/ s11581-023-05110-y

[18] N.Duraisamy, K.Kandiah., R.Rajendran (2018) Electrochemical and photocatalytic investigation of nickel oxide for energy storage and wastewater treatment, *Res Chem Intermed* .,**44**, 5653–5667 . https://doi.org/10.1007/s11164- 018-3446-5

[19] S.A.Soomro, I.H.Gul, H.Naseer, S.Marwat (2019) Improved Performance of CuFe2O4/rGO Nanohybrid as an Anode Material for Lithium-ion Batteries Prepared Via Facile One-step Method, Current Nanoscience., 4, 15, 420-429(10). https://doi.org/10.2174/1573413714666181115122016 10.

[20] P .A .Mikhaylov, M. I. Vinogradov , I .S .Levin, G. A. Shandryuk, A.V.Lubenchenko, V.G.Kulichikhin (2019) Synthesis and characterization of polyethylene terephthalate reduced graphene oxide composites, IOP Conf. Series: Materials Science and Engineering., 693, 012036. 10.1088/1757-899X/693/1/012036.

[21] Y.Zhang , Y.Shen , X.Xie , W.Du, L. K,Y,Wang , X. Sun , Z.Li , B.Wang (2020)One-step synthesis of the reduced graphene oxide@NiO composites for supercapacitor electrodes by electrode-assisted plasma electrolysis, Materials & Design., 196,109111. https://doi.org/10.1016/j.matdes. 2020. 109111

[22] T.G. Vladkova, I.A.Ivanova , A. D. Staneva , M. G. Albu, A.S. A. Shalaby , T. I. Topousova, A. S. Kostadinova (2017) Preparation and Biological Activity of New Collagen Composites Part II: Collagen/Reduced Graphene Oxide Composites, Journal of Archives in Military Medicine.,5, 1 e13223. doi: 10.1007/s12010-016- 2092-x.

[23] J.Xu , L.Wu, Y.Liu et al. (2020) NiO-rGO composite for supercapacitor electrode, Surfaces and Interfaces., 18, 100420 . https://doi.org/10.1016/ j.surfin.2019.100420

[24] T.R.Madhura, G.G.Kumar, R.Ramaraj (2020) Reduced graphene oxide supported 2D-NiO nanosheets modified electrode for urea detection, J Solid State Electrochem, 24, 3073–3081. https://doi.org/10.1007/s10008-020-04763-3

[25] H.Zhu, X.Zeng (2019) A nickel oxide nanoflakes/reduced graphene oxide composite and its high-performance lithium-storage properties, J Solid State Electrochem., 23, 2173–2180 . https://doi.org/10.1007/s10008-019-04281-x

[26] B.S.Singu, K.R.Yoon (2017) Synthesis and characterization of MnO_2- decorated graphene for supercapacitors. Electrochimica Acta., 231, 749-758. https://doi.org/10.1016/j.electacta.2017.01.182

[27] A.Khana , H. Wangb , Y. Liub (2018) Highly Efficient α-Mn2O3@α-MnO2-500 nanocomposite for Peroxymonosulfate Activation: Comprehensive Investigation of Manganese Oxides, J. Mater. Chem., A.6**,** 1590-1600. https://doi.org/10.1039/ C7TA07942G

[28] P.J.S.Jennifer, S.Muthupandi, M.J.R.Ruban (2022) Interlacing Rod and Sphere Morphology of MnO2 in RGO/NiO/MnO_2 Ternary Nanocomposites for Supercapacitive Applications,J. Electrochem. Soc., 169 ,12350.**DOI** 10.1149/1945- 7111/aca8d0 J Solid State Electrochem., 24 30, 5222–5232.

[29] K. M. Racik, K.Guruprasad, M. Mahendiran (2019) Enhanced electrochemical performance of MnO_2/NiO nanocomposite for supercapacitor electrode with excellent cycling stability, Int.J.Energy Research, 46(12), 17163-17179. https://doi.org/10.1007/s10854-019-00821-3

[30] S.G.Hwang, J.E.Hong, G.O.Ki, H.M.Jeong (2012) Graphene Anchored with NiO-MnO_2 Nanocomposites for Use as an Electrode Material in Supercapacitors, ECS Solid State Letters., 2(1): M8-M11.DOI:10.1149/2.010301ssl

[31] E.Liu, W.Li, J.Li (2009) Preparation and characterization of nanostructured NiO/MnO_2 composite electrode for electrochemical super capacitors, Materials Research Bulletin., 44,5, 6:1122-1126. https://doi.org/10.1016/ j.materresbull. 2008.10.003

[32] Y.F.Yuan, J.X.Lin, D.Zhang (2017) Freestanding hierarchical NiO/MnO_2 core/shell nanocomposite arrays for high-performance electrochemical energy storage, Electrochimica Acta., 227, 303-309. https://doi.org/10.1016/ j.electacta. 2017.01.002

[33] J.Chen, Y.Huang, C.Li (2016) Synthesis of NiO@MnO_2 core/shell nanocomposites for supercapacitor application, Applied Surface Science 360, 534- 53.DOI:10.1016/j.apsusc.2015.10.187

[34] T.F.Yi, J.Mei, B.Guan (2020) Construction of spherical NiO@MnO_2 with core- shell structure obtained by depositing MnO_2 nanoparticles on NiO nanosheets for high-performance supercapacitor, Ceramics International., 46(1), 421-429 . https://doi.org/10.1016/j.ceramint.2019.08.278

[35] S.Ramesh, K.Karuppasamy, S.Msolli (2017) A nanocrystalline structured NiO/MnO_2@nitrogen-doped graphene oxide hybrid nanocomposite for high performance supercapacitors, New Journal of Chemistry., 24, 373-382. .https://doi.org/10.1039/C7NJ03730A

[36] S.Sivakumar, N. A.Mala (2021) Influence of Variant Temperatures in Optical, Magnetic Properties of NiO Nanoparticles and its Supercapacitor Applications via Precipitation Method, Asian Journal of Chemistry., 33(8), 1783-1790. http://dx.doi.org/10.14233/ajchem.2021.23242

[37] I.Sengupta, S.Chakraborty, M.Talukdar (2018) Thermal reduction of graphene oxide: How temperature influences purity. Journal of Materials Research., 33:4113– 4122. https://doi.org/10.1557/ jmr.2018.338.

[38] A.Al Nafiey, A.Kumar, M.Kumar (2017) Nickel oxide nanoparticles grafted on reduced graphene oxide (rGO/NiO) as efficient photocatalyst for reduction of nitroaromatics under visible light irradiation, Journal of Photochemistry and Photobiology A: Chemistry., 336, 198-207. https://doi.org/10.1016/ j.jphotochem. 2016.12.023

[39] K. Mohamed Racik, K.Guruprasad, M. Mahendiran (2019) Enhanced electrochemical performance of MnO_2/NiO nanocomposite for supercapacitor electrode with excellent cycling stability, Journal of Materials Science: Materials in Electronics., **30**, 5222–5232. https://doi.org/10.1007/s10854-019 - 00821 - 3

[40] F.Zheng,W.L. Xu, D.Jin (2015) Charge transfer from poly(3-hexylthiophene) to graphene oxide and reduced graphene oxide, RSC Advances., 5(109), 89515- 89520.doi: 10.1039/C5RA18540H.

[41] P.Vijaya Kumar, A.Jafar Ahamed, M. Karthikeyan (2019) Synthesis and characterization of NiO nanoparticles by chemical as well as green routes and their comparisons with respect to cytotoxic effect and toxicity studies in microbial and MCF-7 cancer cell models, SN Appl. Sci., **1**, 1083 . https://doi.org/10.1007/s42452- 019-1113-0 https://doi.org/10.1007/s42452-019-1113-0

[42] Y.Deng, W.Tang, W.Li, Y.Chen (2018) MnO_2-nanowire@NiO-nanosheet core- shell hybrid nanostructure derived interfacial Effect for promoting catalytic oxidation activity, Catalysis Today., 308, 58-63. https://doi.org/ 10.1016/j.cattod. 2017.07.007

[43] W.Gul, R.A.Shah (2023) Synthesis of graphene oxide (GO) and reduced graphene oxide (rGO) and their application as nano-fillers to improve the physical and mechanical properties of medium density fiberboard, Front.Mater., Sec.Polymeric and Composite Materials., 10, 784-793. https://doi.org/10.3389/fmats.2023.1206918

[44] V.Manikandan, R.Elancheran, P.Revathi et al. (2021) Synthesis, Characterization, Photocatalytic and Electrochemical Studies of Reduced Graphene Oxide Doped Nickel Oxide Nanocomposites, Asian Journal of Chemistry.,33(2), 411- 422. DOI: 10.14233/ajchem.2021.22979

[45] H.Fei, N. Saha, N.Kazantseva et al. (2017) A Highly Flexible Supercapacitor Based on MnO2/RGO Nanosheets and Bacterial Cellulose-Filled Gel Electrolyte. Materials., 10, 1251. doi:10.3390/ ma10111251

[46] S.S.Mehta, D.Y.Nadargi, M. S.Tamboli et al. (2021) RGO/WO_3 hierarchical architectures for improved H_2S sensing and highly efficient solar-driving photo-degradation of RhB dye, Scientifc Reports., 11, 5023. https://doi.org/10.1038/s41598-021-84416-1.

[47] N.Tiwari, S.Kulkarni (2022) Impact of Current Collector Base on Supercapacitive Performance of Hydrothermally Reduced Graphene Oxide Electrode, ES Energy Environ., 15, 67-75. https://dx.doi.org/10.30919/esee8c614

[48] L.Ma, X.Y.Pei, D.C. Mo, et al. (2019) Facile fabrication of NiO flakes and reduced graphene oxide (NiO/RGO) composite as anode material for lithium-ion batteries, Journal of Materials Science: Materials in Electronics**.,** 30, 5874–5880 https://doi.org/10.1007/s10854-019-00885-1

[49] B.Belay Etana (2019) Functionalization of textile cotton fabric with reduced graphene oxide/MnO_2/polyaniline based electrode for supercapacitor To cite this article before publication, Mater. Res., 6, 125708. https://doi.org/ 10. 1088/2053- 1591/ab669

[50] G. Vinodhkumara, R. Ramyab, M. Vimalanc (2018) Reduced graphene oxide based on simultaneous detection of neurotransmitters, Progress in

Chemical and Biochemical Research., 1 (1), 40-49. DOI: 10.29088/SAMI/PCBR.2018.1.4049

[51] X. Pu,D. Zhao, C.Fu, Z. Chen, S.Cao, C. Wang et al. (2021) Understanding and Calibration of Charge Storage Mechanism in Cyclic Voltammetry Curves, Chem. Int. Ed., 10.1002/anie.202104167. https://doi.org/10.1002/anie.202104167

[52] E.S. Agudosi, E. C.Abdullah, A. Numan et al. (2020) Fabrication of 3D binder- free graphene NiO electrode for highly stable supercapattery, *Sci Rep* 10., 11214 . https://doi.org/10.1038/s41598-020-68067-2

[53] L.G.Beka, X.Bu, X.Li et al. (2019) A 2D metal–organic framework/reduced graphene oxide heterostructure for supercapacitor application, RSC Adv., 9, 36123- 36135.DOI: 10.1039/C9RA07061C

[54] S. Ge, Y.Zonglin, X. Lijing, B. Zhihong (2020) In-situ conversion of Ni_2P/rGO from heterogeneous self-assembled NiO/rGO precursor with boosted pseudocapacitive performance, Chinese Chemical Letters., 31(6), 1392- 1397. doi: 10.1016/j.cclet.2020.03.046

[55] S. Abbas, S. Manzoor, M.Abdullah (2022) One-pot synthesis of reduced graphene oxide-based PANI/MnO_2 ternary nanostructure for high-efficiency supercapacitor applications ,Journal of Materials Science: Materials in Electronics **., 33**, 25355–25370 (2022). https://doi.org/10.1007/s10854-022-09242-1

[56] N.H. N. Azman. Y.Sulaiman, M.D. S.Mamat (2019) Novel poly(3,4- ethylenedioxythiophene)/reduced graphene oxide incorporated with manganese oxide/iron oxide for supercapacitor device, Journal of Materials Science: Materials in Electronics., **30** , 1458–1467 .https://doi.org/10.1007/s10854-018-0415-0, 2018

[57] Y.Ming, W.C.H. Zhang (2022) Reduced Graphene Oxide Derived from Low-Grade Coal for High-Performance Flexible Supercapacitors with Ultrahigh Cyclability, *Nanomaterials. 12*(17), 2989. https://doi.org/10.3390/nano12172989

[58] L.Lu , S. Xu , J. An , S. Yan (2016) Electrochemical performance of CNTs/RGO/MnO2 composite material for supercapacitor, Nanomaterials and Nanotechnology, 6, 1–7. https://doi.org/10.1177/1847980416663687

[59] J.Huang,F. Li,B. Liu , P. Zhang (2020) Ni_2P/rGO/NF Nanosheets As a Bifunctional High-Performance Electrocatalyst for Water Splitting, Materials .,13(3), 744. https://doi.org/10.3390/ma13030744

[60] Y.S.Chen, C.C.Hu (2003) Capacitive Characteristics of Binary Manganese- Nickel Oxides Prepared by Anodic Deposition ,Electrochem Solid-State Lett.,6, A210–A213. https://doi.org/ 10.1149/1.1601373.

[61] H. Pang, J. Deng, S. Wang, S. Li, J. Du, J. Chen, J. Zhang (2012) Facile synthesis of porous nickel manganite materials and their morphology effect on electrochemical properties, RSC Adv., 2, 5930–5934. https://doi.org/10.1039/C2RA20245J

[62] J. Zhou, X. Shen, M. Jing (2006) Nanosized Ni-Mn Oxides Prepared by the Citrate Gel Process and Performances for Electrochemical Capacitors, J. Mater. Sci. Technol., 22, 803–806. **DOI** 10.1149/1.1541675

[63] H.Kim, B.N.Popov (2003) Synthesis and Characterization of MnO2-Based Mixed Oxides as Supercapacitors, J. Electrochem., Soc., 150, D56–D62. https://doi.org/10.1021/cm0630800

[64] C. H. Wu, J. S. Ma, C. H. Lu (2012) Synthesis and characterization of nickel– manganese oxide via the hydrothermal route for electrochemical capacitors,Curr. Appl. Phys., 12, 1190–1194. https://doi.org/10.1016/j.cap.2012.02.056

[65] H.Jiang, C.Li, T.Sun, J.Ma (2012) Chem High-performance supercapacitor material based on $Ni(OH)_2$ nanowire-MnO_2 nanoflakes core–shell nanostructures,Commun., 48, 2606–2608. https://doi.org/10.1039/C2CC18079K

[66] D.L.Fang, B.C.Wu, Y.Yan, A.Q.Mao, C.H.Zheng (2012) Enhanced supercapacitor performance by incorporating nickel in manganese oxide ,J. Solid State Electrochem., 16, 135–142.

[67] E. H. Liu, W. Li, J. Li, X. Y. Meng, R. Ding, S. T. Tan (2009) Progress in Research on Manganese Dioxide Electrode Materials for Electrochemical Capacitors,Mater. Res. Bull., 44, 1122–1126.

[68] C. Zhu, S. Guo, Y. Fang, L. Han, E. Wang, S. Dong (2011) One-step electrochemical approach to the synthesis of Graphene/MnO_2 nanowall hybrids,Nano Res., 4, 648–657. https://doi.org/10.1016/ S1872-2040(11)60534-3

[69] Z.Lei, F. Shi, L.Lu (2012) Incorporation of MnO_2-Coated Carbon Nanotubes between Graphene Sheets as Supercapacitor Electrode, ACS Appl. Mater. Interfaces., 4, 1058–1064. https://doi.org/10.1021/am2016848

[70] J. Zhu, J. He (2012) Facile Synthesis of Graphene-Wrapped Honeycomb MnO_2 Nanospheres and Their Application in Supercapacitors. Mater. Interfaces, ACS Appl., 4, 1770–1776. https://doi.org/10.1021/am3000165

[71] Y.Jiang, D.Chen, J. Song, Z. Jiao, Q. Ma, H. Zhang, L. Cheng, B. Zhao, Y. Chu (2013) Synthesis of Shape-Controlled NiO/Graphene Nanocomposites with Enhanced Supercapacitive Properties ,Electrochim. Acta., 91, 173–178.

[72] G. Yu, L. Hu, M. Vosgueritchian, H. Wang, X. Xie, J. R. McDonough, X. Cui, Y. Cui, Z. Bao (2011) Solution-Processed Graphene/MnO_2 Nanostructu-red Textiles for High-Performance Electrochemical Capacitors, Nano Lett., 11, 2905 – 2911. https://doi.org/10.1021/nl2013828

IZVOD

NiO/MnO_2 NANOKOMPOZIT KAO DODATAK SLOJEVITOJ ELEKTRODI SA REDUKOVANIM GRAFEN OKSIDOM (RGO) ZA ODGOVORNU PRIMENU SUPERKONDENZATORA

Smanjeni grafen oksid/nikl oksid/magnezijum dioksid, RGO/NiO/MnO_2, nanokompozitna elektroda je uspešno pripremljena jednostavnom metodom ko- precipitacije. Sintetizovani nanokompozit je okarakterisan XRD, FESEM, EDAX, FTIR, UV, CV, GCD, EIS. Nanokompozit RGO/NiO/MnO_2 je prethodno obrađen ultrazvukom, nakon čega je usledilo termičko žarenje na 350°C. Kristalna površina i veličina nanokompozita su analizirani rendgenskom difrakcijom (XRD). Struktura nalik na sendvič RGO/NiO/MnO_2 je analizirana skenirajućim elektronskim mikroskopom (SEM). Ova struktura je promovisala efikasan kontakt između elektrolita i aktivnih materijala, a posebna arhitektura bi mogla da ponudi brze kanale za prenos jona i elektrona. Nanokompozit je pokazao visoku provodljivost zahvaljujući prisustvu RGO. Elektrohemijske performanse pripremljenog nanokompozita urađene su cikličkom voltametrijom (CV), galvanostatskim pražnjenjem naelektrisanja (GCD), spektroskopijom električne impedanse (EIS). Sintetizovani nanokompozit RGO/NiO/MnO_2 dobija visoku specifičnu kapacitivnost od 1167F/g pri gustini struje od 1 A/g. Niskotemperaturna RGO/NiO/MnO_2 nanokompozitna elektroda bi mogla biti elektroda koja obećava za uređaje za skladištenje energije.

Ključne reči: *Redukovani grafen oksid (RGO), nanokompozit NiO/MnO_2, pseudokondenzator, ciklični voltamogrami, superkondenzator.*

Naučni rad
Rad primljen: 03.12.2023.
Rad korigovan: 14.01.2024.
Rad prihvaćen: 16.01.2024
Rad je dostupan na sajtu: www.idk.org.rs/casopis